

# A central role for the lateral prefrontal cortex in goal-directed and stimulus-driven attention

Christopher L Asplund<sup>1</sup>, J Jay Todd<sup>1,2</sup>, Andy P Snyder<sup>1</sup> & René Marois<sup>1</sup>

**Attention is the process that selects which sensory information is preferentially processed and ultimately reaches our awareness. Attention, however, is not a unitary process; it can be captured by unexpected or salient events (stimulus driven) or it can be deployed under voluntary control (goal directed), and these two forms of attention are implemented by largely distinct ventral and dorsal parieto-frontal networks. For coherent behavior and awareness to emerge, stimulus-driven and goal-directed behavior must ultimately interact. We found that the ventral, but not dorsal, network can account for stimulus-driven attentional limits to conscious perception, and that stimulus-driven and goal-directed attention converge in the lateral prefrontal component of that network. Although these results do not rule out dorsal network involvement in awareness when goal-directed task demands are present, they point to a general role for the lateral prefrontal cortex in the control of attention and awareness.**

Reading this manuscript requires attention to be voluntarily deployed, in a ‘top-down’ fashion, to this task. As a consequence of selectively attending to the page, one might become oblivious to surrounding sounds and sights. However, if a fire alarm suddenly blares, this salient stimulus will probably capture attention in a ‘bottom-up’ manner and interrupt the ongoing task so that an appropriate course of action can be initiated. This simple example illustrates a fundamental aspect of attention: what ultimately reaches our awareness and guides our behavior depends on the interaction between goal-directed and stimulus-driven attention<sup>1,2</sup>.

Although much is known about the neural mechanisms that support goal-directed<sup>1,3–7</sup> and stimulus-driven attention<sup>1,5,8–12</sup>, how these two forms of attention are ultimately coordinated is not yet understood. The finding that these attentional forms are supported by largely distinct neural networks, with a dorsal network that includes the frontal eye field (FEF) and superior parietal cortex<sup>1,4–7,13</sup> supporting goal-directed attention and a ventral one that consists of the lateral and inferior frontal/prefrontal cortex and the temporo-parietal junction (TPJ) underlying stimulus-driven attention<sup>1,3,8,9,12,13</sup>, has further complicated the issue. As a result, several hypotheses have been proposed to explain how these two forms of attention might be coordinated: through an interaction between the ventral and dorsal networks<sup>1</sup>, across the dorsal<sup>14,15</sup> or ventral<sup>5</sup> attention network, or in the anterior component of the ventral network<sup>16</sup>. However, many of these proposals are based on studies that used tasks that conflate stimulus-driven and goal-directed attention, thereby making it difficult to determine the relative contributions of bottom-up and top-down neural processes to task performance. For example, the brain mechanisms of stimulus-driven attention cannot easily be dissociated from those of goal-directed behavior if the stimulus-driven attention task involves spatial shifts of attention, goal-oriented processes, or motor responses, as none of these

cognitive processes is necessary to capture attention exogenously but all are known to engage the dorsal attentional network<sup>1,3–6</sup>.

The same concern also applies to our current understanding of how attention controls awareness. Both the ventral and dorsal attentional networks have been associated with conscious perception<sup>5,17–23</sup>, lending support to theories of awareness in which widespread changes in brain activity accompany conscious perception<sup>17,24</sup>. However, there has been no specific attempt to assess the relative contributions of the dorsal and ventral networks to the neural basis of attentional limits to conscious perception by using tasks that dissociate between stimulus-driven and goal-directed attentional processes. Hence, the extent to which each of these attention networks is necessary for awareness is currently unclear<sup>22,23,25</sup>.

We have recently developed an experimental procedure that reveals a profound but fleeting deficit in visual awareness resulting from the foveal presentation of an unexpected, task-irrelevant stimulus that involves neither an overt response nor a shift in spatial attention. The deficit, termed surprise-induced blindness (SiB), is triggered by an event that is absent from the observer’s goal-directed attentional set and is not under the observer’s initial control<sup>26</sup>. As such, the procedure represents a powerful way to assess whether stimulus-driven attentional limits to conscious perception can arise within the ventral attention network in the absence of dorsal network involvement. Moreover, because the unexpected event ultimately affects the goal-directed task of detecting a target, SiB experiments are also well suited to reveal the neural mechanisms by which stimulus-driven attention affects goal-directed behavior.

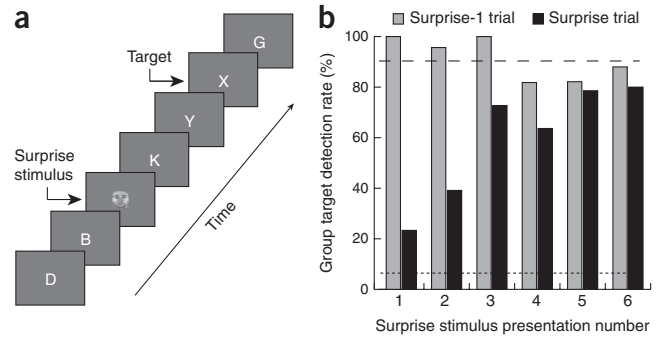
## RESULTS

We scanned 30 participants while they were searching for a target in a rapid serial visual presentation (RSVP) stream of distractor

<sup>1</sup>Department of Psychology, Vanderbilt Vision Research Center, Vanderbilt University, Nashville, Tennessee, USA. <sup>2</sup>Department of Psychology, University of Chicago, Chicago, Illinois, USA. Correspondence should be addressed to C.L.A. (chris.asplund@vanderbilt.edu) or R.M. (rene.marois@vanderbilt.edu).

Received 16 September 2009; accepted 29 January 2010; published online 7 March 2010; corrected online 14 March 2010 (details online); doi:10.1038/nn.2509

**Figure 1** SiB experiment (Experiment 1). (a) Trial design. Participants searched for a target letter in a rapid serial visual presentation (RSVP) stream of distractor letters. In a small proportion of trials (surprise trials), a surprise face stimulus was shown before the target. (b) Group target detection performance. Black bars represent accuracy in surprise trials, and gray bars represent accuracy in trials immediately preceding the surprise trials (surprise-1). Dashed line corresponds to the average target hit rate for search trials (target only). Dotted line corresponds to the false alarm rate.



items (**Fig. 1a**). Unannounced to the participants, a salient but task-irrelevant stimulus occurred 330 ms before the target in a small proportion of trials (surprise trials), causing SiB (**Fig. 1b**). Specifically, group target detection performance differed across the surprise stimuli presentations (Cochran's  $Q_4 = 30.3$ ,  $P < 0.0001$ ; see Online Methods), with target detection worse following the first surprise trial (SS1) than after SS3–SS6 (sign tests,  $P$ 's  $< 0.040$ ; see Online Methods), and worse after SS2 than after SS5 or SS6 ( $P$ 's  $< 0.027$ ). In SS3–SS6, performance was comparable to search trials (trials without surprise stimuli, for which the target detection rate was 90.4%; **Fig. 1b**). Target-detection performance in the trials immediately preceding the first two surprise trials was far better than in the respective surprise trials (sign tests,  $P$ 's  $< 0.0001$ ; **Fig. 1b**), indicating that SiB does not result from an initial difficulty with the target detection task. Rather, the finding that unexpected, task-irrelevant stimuli triggered a profound but short-lived impairment in target detection that was essentially dissipated by the third surprise stimulus presentation is consistent with a stimulus-driven, attention-based origin for this deficit<sup>26</sup>.

### Neural correlates of SiB

To identify the neural substrates that underlie stimulus-driven attentional limits to conscious perception, we first isolated the brain regions that were sensitive to the surprise stimuli, irrespective of presentation number (see Online Methods). We then examined the BOLD (blood-oxygen-level dependent) signal from these brain regions,

testing whether the response pattern mirrored the behavioral performance. Specifically, because presentations of rare, task-irrelevant stimuli are known to increase neural activity<sup>8–10,27</sup> and because SiB was only observed for the first pair of surprise stimuli (SS1+2), we predicted that this pair would cause a greater BOLD response than the two subsequent pairs (SS3+4 and SS5+6) of surprise stimuli (the time courses from each consecutive pair of surprise stimuli were averaged to improve statistical power; see Online Methods).

A statistical parametric map (SPM) revealed several brain areas that were recruited more during surprise than during search trials (**Table 1**, **Fig. 2** and **Supplementary Fig. 1**). Several of these areas showed invariant BOLD responses across the six surprise stimuli presentations, most notably the fusiform gyrus in visual cortex, suggesting that SiB might be a primarily central phenomenon that occurs at later stages than visual information processing. Correspondingly, the only two regions that demonstrated a BOLD response that quickly habituated after the first two surprise stimulus presentations were in association cortex (**Fig. 2**): the inferior frontal junction (IFJ), located in the posterior aspect of the inferior frontal sulcus (parts of Brodmann areas 9, 44, 6), and the temporo-parietal junction (TPJ), at the intersection of the superior temporal gyrus, supramarginal gyrus and superior temporal sulcus (parts of

**Table 1** Anatomical location and statistical assessment of activation for the ROIs isolated from surprise trials in Experiment 1 (surprise trial–search trial contrast)

| Region        | Hemi      | Talairach coordinates (x, y, z) | SS1+2 vs. SS3+4 (t) | SS3+4 vs. SS5+6 (t) | SS1+2 vs. SS5+6 (t) |
|---------------|-----------|---------------------------------|---------------------|---------------------|---------------------|
| TPJ           | Right     | 46, -56, 27                     | 2.11*               | 1.07                | 2.76*               |
| TPJ           | Left      | -49, -56, 23                    | 2.35*               | 1.30                | 2.86*               |
| IFJ           | Right     | 37, 5, 29                       | 2.72*               | -0.37               | 2.05*               |
| IFJ           | Left      | -40, 8, 25                      | 2.46*               | 0.05                | 2.18*               |
| FG            | Right     | 30, -44, -11                    | 0.42                | -0.92               | -0.53               |
| FG            | Left      | -32, -51, -10                   | 1.05                | -0.70               | 0.05                |
| IFG           | Right     | 40, 19, 13                      | 0.75                | 0.30                | 1.09                |
| IFG           | Left      | -48, 19, 7                      | -0.57               | 0.77                | 0.19                |
| OFC           | Right     | 34, 27, -10                     | -0.22               | -0.19               | -0.53               |
| OFC           | Left      | -37, 26, -8                     | 0.27                | 0.15                | 0.40                |
| Pulvinar      | Bilateral | -7/9, -27, 1                    | 1.46                | 0.71                | 1.83                |
| PG            | Right     | 32, -3, -13                     | -0.09               | -0.70               | -0.80               |
| STG           | Right     | 33, 12, -27                     | 0.95                | 0.07                | 1.26                |
| MTS           | Left      | -51, 2, -12                     | -0.17               | -0.28               | -0.36               |
| SFG           | Right     | 13, 24, 49                      | 0.49                | 0.74                | 0.90                |
| Amygdala/SLEA | Right     | 16, -9, -8                      | 1.58                | -0.17               | 1.26                |

The three rightmost columns list the  $t$ -values resulting from paired  $t$ -tests of the given surprise stimulus pairs. Amygdala/SLEA, amygdala and sublentiform extended amygdala; FG, fusiform gyrus (Brodmann area 37); IFG, inferior frontal gyrus (Brodmann areas 44, 45); IFJ, inferior frontal junction (Brodmann areas 9, 44, 6); MTS, middle temporal sulcus (Brodmann area 21); OFC, orbitofrontal cortex (Brodmann area 47); PG, parahippocampal gyrus; SFG, superior frontal gyrus (Brodmann area 8); STG, superior temporal gyrus (Brodmann area 38)<sup>45</sup>; TPJ, temporo-parietal junction (Brodmann areas 39, 40, 22). With the exception of the IFJ and TPJ, none of these brain regions showed activation differences between any of the three surprise stimulus pairs (all  $P$ 's  $> 0.1$ ), although the amygdala/SLEA and pulvinar showed non-significant trends for greater SS1+2 activation relative to the two other SS pairs. Note that the TPJ foci are anatomically distinct from, and superior to, regions of the superior temporal sulcus involved in processing facial expressions and eye gaze<sup>46</sup>.

\* $P < 0.05$ .

Brodmann areas 40, 22, 39). For these two brain regions, in both hemispheres, the peak response to SS1+2 was higher than the response to the two other SS pairs (two-tailed paired  $t$  tests,  $t_{29}$ 's  $> 2.05$ ,  $P$ 's  $< 0.049$ ), whereas the peak responses to SS3+4 and SS5+6 were indistinguishable ( $t_{29}$ 's  $< 1.30$ ,  $P$ 's  $> 0.20$ ; **Fig. 2**). Thus, the IFJ and TPJ exhibited an activity pattern that mirrored the magnitude of SiB. This activity modulation was caused by the surprise stimuli, not the perceived absence of a target, which co-varies with SiB, because the peak responses in target-absent trials and search trials (see Online Methods) were indistinguishable (two-tailed paired  $t$  tests,  $t_{29}$ 's  $< 1.17$ ,  $P$ 's  $> 0.25$ ). No other brain regions showed an SiB-like pattern of activation, as an additional SPM that directly contrasted SS1+2 with SS3+4 and SS5+6 demonstrated.

Together, these results indicate that the presentation of unexpected, task-irrelevant stimuli activates a large network of cortical and subcortical regions, but only a subset of this network in the frontal/prefrontal and temporo-parietal cortex shows a rapid BOLD response adaptation that is commensurate with the behavioral performance. This subset

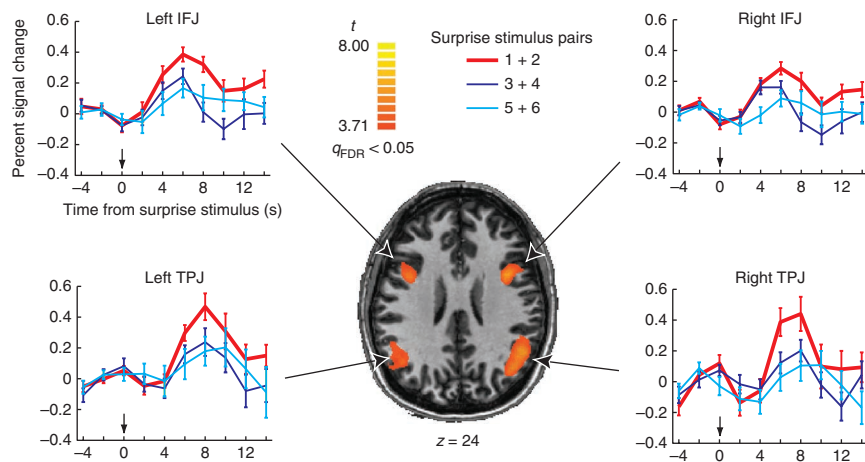


**Figure 2** SiB experiment (Experiment 1) SPM. Brain regions showing rapid attenuation of surprise stimulus-related activation. The SPM highlights brain regions that responded to all six surprise trials (see Online Methods), specifically the IFJs (Talairach coordinates<sup>45</sup> 37, 5, 29 and -40, 8, 25) and TPJs (Talairach coordinates 46, -56, 27 and -49, -56, 23). The time courses illustrate the brain regions from the SPM that showed greater activity in the first pair of Surprise trials than in the two other pairs of surprise trials. The surprise stimulus appears at approximately time zero. Error bars represent s.e.m.

Online Methods and **Fig. 3b**), while activity within each of these two pairs did not differ (all  $P$ 's > 0.55). These results were obtained regardless of whether the IFJ and TPJ ROIs

of brain regions is anatomically consistent with areas previously implicated in novelty processing<sup>8,9,11,27–30</sup>, attentional orienting to sensory events<sup>31,32</sup> and, most notably, to the core components of the ventral attention network<sup>1,13</sup>.

### Late dorsal network activation

In contrast to the ventral network, the SPMs (even with a liberal threshold of  $P < 0.001$ , uncorrected) provided no evidence for surprise stimulus-related activation in the core brain regions associated with the goal-directed attention network<sup>1,13</sup>, namely the frontal eye field (FEF) and the intraparietal sulcus (IPS). To analyze the dorsal network's association with SiB with greater sensitivity, for each participant, we functionally defined regions of interest (ROIs) for the putative FEF and IPS based on their activation in search trials, as these regions were strongly activated by the task of searching for and responding to targets (see Online Methods, **Fig. 3** and **Table 2**). The anatomical locations of the resulting ROIs corresponded well to the conventional positions of the FEF and IPS in goal-directed attention tasks<sup>1,3–6,12,13,16</sup>. When probed during the surprise trials, activity in these dorsal regions was greater during SS1+2 than in search trials ( $t_{29}$ 's > 2.50,  $P$ 's < 0.018 except for a marginal effect in the right FEF at  $t_{29} = 1.79$ ,  $P = 0.084$ ) but not during subsequent pairs (**Table 2**). Thus, the more sensitive ROI analysis revealed that the FEF and IPS are also activated by the first two surprise stimulus presentations. Notably, however, the time courses of activation specific to the first pair of surprise stimuli, revealed by subtracting the underlying search-related activity from the first two surprise stimulus trials (see Online Methods), showed that the IPS and FEF responded significantly later than did the IFJ and TPJ (all pair-wise comparisons  $P < 0.048$ ; see

were defined exactly as the IPS and FEF ROIs or on the basis of the group-level surprise trial ROIs (**Tables 1** and **2**).

Thus, the ROI analysis revealed that the dorsal network is activated by the surprise stimuli, but unlike the swift activation pattern in the ventral network following presentations of the first two surprise stimuli, the dorsal network appears to respond too late (by about 3 s) for it to cause SiB. However, this conclusion depends on the dorsal activation delay reflecting a genuine late neural response rather than inherent differences in the hemodynamic properties of the ventral and dorsal parieto-frontal networks. We performed a follow-up 'spatial SiB' experiment (Experiment 2) to distinguish between these possibilities. Given the role of the dorsal network in the control of visuo-spatial attention<sup>1,4,6</sup>, we predicted that the sporadic presentations of highly salient, categorically distinct task-irrelevant stimuli in the periphery instead of in the center of the RSVP stream (**Fig. 4a**) would not only persist in capturing attention<sup>26</sup> but also lead to shifts of visual-spatial attention or eye movements, thereby promptly recruiting the FEF and IPS in addition to the ventral network. Consistent with our hypothesis, we found a persistent SiB effect and robust activations in both the dorsal and ventral networks (**Fig. 4b**, and **Supplementary Tables 1** and **2**). Notably, there was no longer a delay in activation between the dorsal and ventral networks ( $P$ 's > 0.36), in marked contrast to Experiment 1 (timing delay difference across experiments: one-tailed  $P = 0.038$ ; see Online Methods). These results indicate that the delay in activation of the dorsal brain regions during the surprise trials of Experiment 1 had a neural, not hemodynamic, origin. Additional behavioral evidence indicates that this delayed activation might reflect the modulation of top-down attentional settings in anticipation of post-surprise stimulus trials

**Figure 3** Stimulus-driven and goal-directed attention activity in Experiment 1. **(a)** Dorsal brain regions that are active during search trials. **(b)** Surprise stimulus-specific waveform in dorsal (FEF, IPS) and ventral (IFJ, TPJ) regions of interest (ROIs) defined in individual participants (see Online Methods). Each time course was constructed by subtracting the search trial time course from the time course for the first two surprise stimulus trials. The surprise stimulus appears at approximately time zero. **(c)** Search trial activation time course over the same period of time as in **b** for the same ROIs. Arrows mark each trial's onset. Note that the activation pattern is cyclical, mirroring the trial structure (one trial every 8 s). The observed hemodynamic responses in IPS, FEF and IFJ match the predicted responses for the hypothesized search-related activity (**Supplementary Fig. 3**).

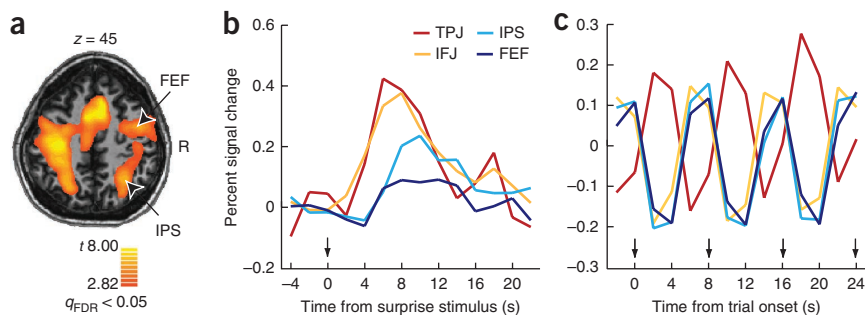


**Table 2 Average anatomical location and statistical assessment of activation for the individually defined ROIs from search trials in Experiment 1 (open contrast SPM)**

| Region | Hemi  | Talairach coordinates<br>(x, y, z) ± s.d. | SS1+2 vs.<br>search (t) | SS3+4 vs.<br>search (t) | SS5+6 vs.<br>search (t) |
|--------|-------|---|-------------------------|-------------------------|-------------------------|
| IPS    | Right | 26 ± 4, -65 ± 6, 36 ± 5                   | 2.81*                   | 0.46                    | 0.28                    |
| IPS    | Left  | -22 ± 4, -66 ± 6, 39 ± 6                  | 3.45*                   | 0.44                    | 1.38                    |
| FEF    | Right | 34 ± 4, -7 ± 3, 51 ± 5                    | 1.79                    | 0.51                    | 0.63                    |
| FEF    | Left  | -32 ± 5, -8 ± 3, 51 ± 5                   | 2.50*                   | 1.95                    | 0.96                    |
| TPJ    | Right | 47 ± 5, -55 ± 5, 28 ± 5                   | 4.52*                   | 3.21*                   | 1.65                    |
| TPJ    | Left  | -49 ± 2, -58 ± 5, 24 ± 4                  | 5.33*                   | 2.37*                   | 1.73                    |
| IFJ    | Right | 40 ± 4, 6 ± 3, 27 ± 3                     | 4.99*                   | 1.67                    | 1.06                    |
| IFJ    | Left  | -42 ± 3, 8 ± 3, 25 ± 2                    | 5.92*                   | 2.51*                   | 1.12                    |

The three rightmost columns list the *t*-values resulting from paired *t*-tests of the given surprise stimulus pairs versus target-only activity. See **Table 1** for abbreviations. These ROI coordinates closely matched those isolated from the surprise trials (**Table 1**).

\**P* < 0.05.

(**Supplementary SiB RT Experiment** and **Supplementary Fig. 2**). Regardless of the function of this delayed dorsal response to surprise stimulus presentations, it does not appear to be involved in SiB, as the FEF and IPS are activated after the events that trigger the perceptual deficit.

### Interaction of goal-directed and stimulus-driven attention

If the core components of the dorsal attentional network (the FEF and IPS) are not responsible for SiB, then how do the surprise stimuli ultimately impair the goal-directed task of searching for and responding to a target? That is, how does stimulus-driven attention disrupt goal-directed behavior? The answer is provided by an examination of the temporal dynamics of activation in the two attentional networks during the search trials of Experiment 1. In these trials, the FEF and IPS showed the pattern expected of brain regions associated with goal-directed behavior, namely an activation profile that tightly correlated with performing the primary search task (**Fig. 3c**). By contrast, TPJ activity was out of phase with activity in the dorsal brain regions, showing deactivation when the others were activated (onset shifts of ~4 s, *P*'s < 0.0001; **Fig. 3c**), consistent with the finding that attention-demanding cognitive tasks are often accompanied by suppression of TPJ activity<sup>13,21,33–35</sup>. Notably, the time course of IFJ activity no longer closely followed that of its ventral network cohort, the TPJ (onset shifts of ~4 s, *P*'s < 0.0001), but instead closely tracked the activation time course of the dorsal brain regions (**Fig. 3c**). This IFJ activity in the search trials does not simply reflect target detection, for the same activity pattern was found in target-absent trials. These findings suggest that the IFJ might be not only a core member of the ventral attention network that supports stimulus-driven attention, but also functionally integrated with the dorsal network during goal-directed behavior.

To test the hypothesis that the IFJ ROIs identified in Experiment 2 are important in goal-directed behavior, we carried out an additional experiment (Experiment 3) that assessed whether the IFJ is activated, along with the FEF and IPS, in a prototypical goal-directed attention task, an endogenous Posner cueing task<sup>3,36</sup> (**Fig. 5a**; see Online Methods). In this task, participants made a speeded response to a target presented at a location that was cued by the color of a central fixation point, with the cue validly predicting the location of the target on 80% of the trials. The task was successful in engaging goal-directed attention, evidenced by the fact that participants were faster at detecting the target at validly cued than at invalidly cued positions (reaction time ± s.d., 317 ± 36 ms versus 396 ± 64 ms, *t*<sub>5</sub> = 4.53, *P* = 0.0062). The dorsal brain regions were activated

during the cue-related period (*t*<sub>5</sub>'s > 3.53, *P*'s < 0.017; see Online Methods), as expected of brain regions involved in goal-directed attention<sup>1,3,6</sup> (**Fig. 5b**). Furthermore, the IFJ was also activated by the cue (*t*<sub>5</sub> = 2.74, *P* = 0.041) and at the same time as the FEF and IPS. These results were obtained regardless of whether the ROIs were defined in the cueing task or in the search trials of the RSVP task, attesting to the fact that the brain regions that showed goal-directed activity in the search trials are also involved in visuo-spatial shifts of attention. We therefore conclude that IFJ supports goal-directed behavior, as it is activated along with core members of the dorsal network during the cue period of a classic goal-directed attention task. These conclusions are consistent with previous reports suggesting that similar brain regions are activated in other cued attention shift tasks<sup>37,38</sup>.

Together, the results of our experiments indicate that the IFJ participates in both stimulus-driven and goal-directed attention. While the pattern of IFJ activity is consistent with brain regions involved in stimulus-driven attention during the presentation of a surprise stimulus, its activity profile is instead more consistent with those of goal-directed brain regions during the search task. It follows from these results that the IFJ should be more functionally integrated with core members of the dorsal network during goal-directed attention but with core members of the ventral network during stimulus-driven attention. These predictions were borne out by a functional connectivity analysis (see Online Methods), which showed that IFJ activity was correlated positively with activity in the FEF and IPS (IFJ-FEF, *t*<sub>29</sub> = 9.13, *P* < 0.0001; IFJ-IPS, *t*<sub>29</sub> = 12.19, *P* < 0.0001; FEF-IPS, *t*<sub>29</sub> = 6.87, *P* < 0.0001), but negatively with TPJ activity (*t*<sub>29</sub> = -4.27, *P* = 0.00019), during the search trials. Conversely, following the presentation of a surprise stimulus, the IFJ-FEF and IFJ-IPS correlations decreased (paired *t* test of the changes: *t*<sub>29</sub> = -2.12, *P* = 0.043; *t*<sub>29</sub> = -2.36, *P* = 0.025), whereas those between IFJ and TPJ increased (*t*<sub>29</sub> = 2.07, *P* = 0.047) and those between FEF and IPS did not change (*t*<sub>29</sub> = -1.07, *P* = 0.29). These connectivity results provide additional evidence that the IFJ underlies stimulus-driven and goal-directed attention, with its response profile and network allegiance depending on task demands. In that context, SiB would result from the 'bottom-up' engagement of IFJ by the presentation of a surprise stimulus, thereby transiently disrupting or altering this brain region's control of the target detection task. With behavioral and neuronal habituation to the repeated surprise stimulus presentations, the IFJ might be able to maintain its goal-oriented activity even in the face of task-irrelevant stimulus presentations.

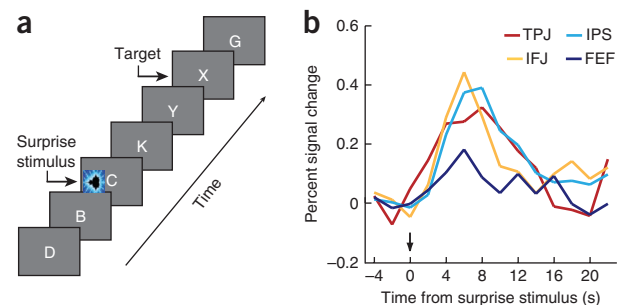


**Figure 4** Spatial SiB experiment (Experiment 2). **(a)** Trial design. The procedure was identical to that in Experiment 1 save that in a small proportion of trials, a colorful surprise stimulus was shown before the target away from fixation (**Fig. 1a**). **(b)** Surprise stimulus-specific waveforms in dorsal and ventral attention network ROIs defined in individual participants. Time courses were constructed in the same fashion as those in Experiment 1 (see **Fig. 3b**). Note that all four regions show an immediate response to the surprise stimulus presentations.

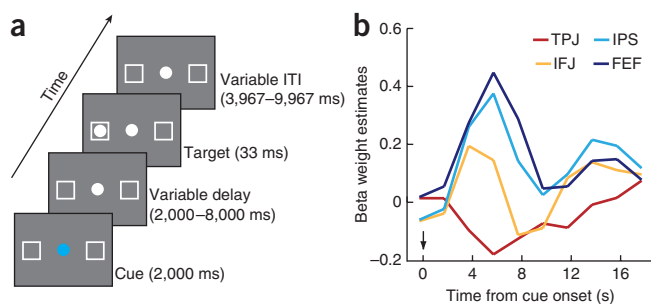


**Figure 5** Endogenous cueing task experiment (Experiment 3). **(a)** Trial design. A color cue predicted the location of an upcoming target, to which the participant then responded in a speeded manner. **(b)** Cue-related activity in dorsal and ventral attention network ROIs isolated from Experiment 2 (see Online Methods). The arrow marks cue onset. ITI, inter-stimulus interval.

## DISCUSSION

Our study reveals that both functional divergence and convergence of the dorsal and ventral attentional networks underlie attention and awareness. Divergence of function between these two networks is clearly shown by the SiB procedure, as it shows that stimulus-driven attentional limits to conscious perception can arise from the ventral attentional network in the absence of dorsal network or visual cortex modulation. In contrast, previous neurobiological investigations<sup>17–22,39,40</sup> have frequently implicated regions of both the ventral and dorsal networks in awareness. Such large-scale activation patterns are consistent with ‘global workspace’ models that posit that awareness emerges from the reverberating activity of a widely distributed cortical network<sup>17,22,24</sup>. The difference in activation patterns between these previous studies and the present one is probably the result of differences in task design. Whereas previous tasks have included spatial shifts of attention<sup>3,5,14,15,18,39</sup> or covert or overt responses<sup>3,5,11,12,18–21,39,40</sup> to the critical attention-capturing stimulus, our task was specifically designed to exclude these components as they are unnecessary for exogenous attentional capture but can activate the dorsal attention network<sup>1,3–6</sup>. As such, our task shows that the dorsal network’s contribution to conscious perception might be negligible under these controlled circumstances. This conclusion is consistent with the suggestion that awareness is not necessarily an emergent property of the dorsal network<sup>25</sup> and poses a challenge to global network theories of awareness.

These conclusions, however, do not imply that the dorsal network never has a role in attentional limits to explicit perception. Dorsal structures might contribute to, and be essential for, conscious perception during tasks that involve top-down or goal-oriented processing, such as change detection or binocular rivalry<sup>17,18,22,40</sup>. Indeed, just as deficits of awareness in different visual domains often have dissociable neural origins (for example, prosopagnosia versus achromatopsia)<sup>22</sup>, awareness might also be fractionated at central, attentional stages of information processing. Additional research, aided by better delineation of the topographically distinct sub-regions of the IPS<sup>41</sup>, will be necessary to assess the specific contributions of the dorsal network to attentional limits to conscious perception and awareness in general.

As well as revealing a functional dissociation between the ventral and dorsal attentional networks in awareness, the very nature of SiB, a profound deficit in the detection of a goal-relevant target as a result of the presentation of an unexpected and task-irrelevant stimulus, underscores that stimulus-driven and goal-directed attention must ultimately interact<sup>1,2,5,13–16</sup>. Our results indicate that the ventral attention network’s lateral prefrontal component, the inferior frontal

junction, is the site of convergence for stimulus-driven and goal-directed attention, a finding that is consistent with recent resting state functional connectivity data suggesting that this brain region functionally interacts with both ventral and dorsal brain structures<sup>16</sup>. The IFJ has also been implicated in task-switching and cognitive control<sup>42,43</sup> more generally. This brain region is therefore ideally suited to act as the neural site of coordination for stimulus-driven and goal-directed attention. Moreover, the IFJ’s involvement in both the non-spatial and spatial SiB tasks (Experiments 1 and 2) indicates that this brain region’s function generalizes across both spatial and non-spatial forms of attention. While it remains to be seen whether all these attentional processes are mediated by the same sub-populations of IFJ neurons, a central role for this brain region in the co-ordination of stimulus-driven and goal-directed attention across both spatial and non-spatial domains resonates well with the proposal that the IFJ is a critical neural substrate that underlies our limited attentional capacities<sup>44</sup>.

## METHODS

Methods and any associated references are available in the online version of the paper at <http://www.nature.com/natureneuroscience/>.

*Note: Supplementary information is available on the Nature Neuroscience website.*

## ACKNOWLEDGMENTS

We thank B. Rogers, J. Swisher and E. Conser. This work was supported by National Science Foundation grant 0094992 and National Institute of Mental Health grant R01 MH70776 (R.M.).

## AUTHOR CONTRIBUTIONS

C.L.A. designed and performed experiments, analyzed data, and wrote the manuscript. J.J.T. and A.P.S. designed and performed experiments. R.M. designed experiments and wrote the manuscript.

## COMPETING FINANCIAL INTERESTS

The authors declare no competing financial interests.

Published online at <http://www.nature.com/natureneuroscience/>.

Reprints and permissions information is available online at <http://www.nature.com/reprintsandpermissions/>.

- Corbetta, M. & Shulman, G.L. Control of goal-directed and stimulus-driven attention in the brain. *Nat. Rev. Neurosci.* **3**, 201–215 (2002).
- Egeth, H.E. & Yantis, S. Visual attention: control, representation, and time course. *Annu. Rev. Psychol.* **48**, 269–297 (1997).
- Corbetta, M., Kincade, J.M., Ollinger, J.M., McAvoy, M.P. & Shulman, G.L. Voluntary orienting is dissociated from target detection in human posterior parietal cortex. *Nat. Neurosci.* **3**, 292–297 (2000).
- Kastner, S., Pinsk, M.A., De Weerd, P., Desimone, R. & Ungerleider, L.G. Increased activity in human visual cortex during directed attention in the absence of visual stimulation. *Neuron* **22**, 751–761 (1999).
- Serences, J.T. *et al.* Coordination of voluntary and stimulus-driven attentional control in human cortex. *Psychol. Sci.* **16**, 114–122 (2005).
- Yantis, S. *et al.* Transient neural activity in human parietal cortex during spatial attention shifts. *Nat. Neurosci.* **5**, 995–1002 (2002).
- Chiu, Y.C. & Yantis, S. A domain-independent source of cognitive control for task sets: Shifting spatial attention and switching categorization rules. *J. Neurosci.* **29**, 3930–3938 (2009).
- Downar, J., Crawley, A.P., Mikulis, D.J. & Davis, K.D. A multimodal cortical network for the detection of changes in the sensory environment. *Nat. Neurosci.* **3**, 277–283 (2000).
- Downar, J., Crawley, A.P., Mikulis, D.J. & Davis, K.D. A cortical network sensitive to stimulus salience in a neutral behavioral context across multiple sensory modalities. *J. Neurophysiol.* **87**, 615–620 (2002).
- Horowitz, S.G., Skudlarski, P. & Gore, J.C. Correlations and dissociations between BOLD signal and P300 amplitude in an auditory oddball task: a parametric approach to combining fMRI and ERP. *Magn. Reson. Imaging* **20**, 319–325 (2002).
- Linden, D.E. *et al.* The functional neuroanatomy of target detection: an fMRI study of visual and auditory oddball tasks. *Cereb. Cortex* **9**, 815–823 (1999).
- Marois, R., Leung, H.C. & Gore, J.C. A stimulus-driven approach to object identity and location processing in the human brain. *Neuron* **25**, 717–728 (2000).
- Corbetta, M., Patel, G. & Shulman, G.L. The reorienting system of the human brain: from environment to theory of mind. *Neuron* **58**, 306–324 (2008).

14. Buschman, T.J. & Miller, E.K. Top-down versus bottom-up control of attention in the prefrontal and posterior parietal cortices. *Science* **315**, 1860–1862 (2007).
15. Gottlieb, J. From thought to action: the parietal cortex as a bridge between perception, action and cognition. *Neuron* **53**, 9–16 (2007).
16. He, B.J. *et al.* Breakdown of functional connectivity in frontoparietal networks underlies behavioral deficits in spatial neglect. *Neuron* **53**, 905–918 (2007).
17. Dehaene, S., Changeux, J.P., Naccache, L., Sackur, J. & Sergent, C. Conscious, preconscious and subliminal processing: a testable taxonomy. *Trends Cogn. Sci.* **10**, 204–211 (2006).
18. Beck, D.M., Rees, G., Frith, C.D. & Lavie, N. Neural correlates of change detection and change blindness. *Nat. Neurosci.* **4**, 645–650 (2001).
19. Rees, G., Russell, C., Frith, C.D. & Driver, J. Inattention blindness versus inattentional amnesia for fixated, but ignored, words. *Science* **286**, 2504–2507 (1999).
20. Marois, R., Chun, M.M. & Gore, J.C. Neural correlates of the attentional blink. *Neuron* **28**, 299–308 (2000).
21. Marois, R., Yi, D.J. & Chun, M.M. The neural fate of consciously perceived and missed events in the attentional blink. *Neuron* **41**, 465–472 (2004).
22. Rees, G., Kreiman, G. & Koch, C. Neural correlates of consciousness in humans. *Nat. Rev. Neurosci.* **3**, 261–270 (2002).
23. Husain, M. & Nachev, P. Space and the parietal cortex. *Trends Cogn. Sci.* **11**, 30–36 (2007).
24. Baars, B.J. In the theatre of consciousness: global workspace theory, a rigorous scientific theory of consciousness. *J. Conscious. Stud.* **4**, 292–309 (1997).
25. Goodale, M.A. & Milner, A.D. Separate visual pathways for perception and action. *Trends Neurosci.* **15**, 20–25 (1992).
26. Asplund, C.L., Todd, J.J., Snyder, A.P., Gilbert, C.M. & Marois, R. Surprise-induced blindness: a stimulus-driven attentional limit to conscious perception. *J. Exp. Psychol. Hum. Percept. Perform.* (in the press).
27. Yamaguchi, S., Hale, L.A., D'Esposito, M. & Knight, R.T. Rapid prefrontal-hippocampal habituation to novel events. *J. Neurosci.* **24**, 5356–5363 (2004).
28. Knight, R.T. Decreased response to novel stimuli after prefrontal lesions in man. *Electroencephalogr. Clin. Neurophysiol.* **59**, 9–20 (1984).
29. Opitz, B., Mecklinger, A., Friederici, A.D. & von Cramon, D.Y. The functional neuroanatomy of novelty processing: integrating ERP and fMRI results. *Cereb. Cortex* **9**, 379–391 (1999).
30. Courchesne, E., Hillyard, S.A. & Galambos, R. Stimulus novelty, task relevance and the visual evoked potential in man. *Electroencephalogr. Clin. Neurophysiol.* **39**, 131–143 (1975).
31. Heilman, K.M. & Watson, R.T. Mechanisms underlying the unilateral neglect syndrome. *Adv. Neurol.* **18**, 93–106 (1977).
32. Karnath, H.O., Milner, A.D. & Vallar, G. *The Cognitive and Neural Bases of Spatial Neglect* (Oxford University Press, Oxford, 2002).
33. Todd, J.J., Fougner, D. & Marois, R. Visual short-term memory load suppresses temporo-parietal junction activity and induces inattentional blindness. *Psychol. Sci.* **16**, 965–972 (2005).
34. Shulman, G.L., Astafiev, S.V., McAvoy, M.P., d'Avossa, G. & Corbetta, M. Right TPJ deactivation during visual search: functional significance and support for a filter hypothesis. *Cereb. Cortex* **17**, 2625–2633 (2007).
35. Fox, M.D. *et al.* The human brain is intrinsically organized into dynamic, anticorrelated functional networks. *Proc. Natl. Acad. Sci. USA* **102**, 9673–9678 (2005).
36. Posner, M.I., Snyder, C.R.R. & Davidson, B.J. Attention and the detection of signals. *J. Exp. Psychol. Gen.* **109**, 160–174 (1980).
37. Corbetta, M. *et al.* A common network of functional areas for attention and eye movements. *Neuron* **21**, 761–773 (1998).
38. Kastner, S. *et al.* Topographic maps in human frontal cortex revealed in memory-guided saccade and spatial working-memory tasks. *J. Neurophysiol.* **97**, 3494–3507 (2007).
39. Huettel, S.A., Güzeldere, G. & McCarthy, G. Dissociating the neural mechanisms of visual attention in change detection using functional MRI. *J. Cogn. Neurosci.* **13**, 1006–1018 (2001).
40. Lumer, E.D., Friston, K.J. & Rees, G. Neural correlates of perceptual rivalry in the human brain. *Science* **280**, 1930–1934 (1998).
41. Konen, C.S. & Kastner, S. Representation of eye movements and stimulus motion in topographically organized areas of human PPC. *J. Neurosci.* **28**, 8361–8375 (2008).
42. Brass, M., Derrfuss, J., Forstmann, B. & von Cramon, D.Y. The role of the inferior frontal junction in cognitive control. *Trends Cogn. Sci.* **9**, 314–316 (2005).
43. Koechlin, E., Ody, C. & Kouneiher, F. The architecture of cognitive control in the human prefrontal cortex. *Science* **302**, 1181–1185 (2003).
44. Marois, R. & Ivanoff, J. Capacity limits of information processing in the brain. *Trends Cogn. Sci.* **9**, 296–305 (2005).
45. Talairach, J. & Tournoux, P. *Co-planar Stereotaxic Atlas of the Human Brain* (Thieme Medical Publishers, New York, 1988).
46. Hoffman, E.A. & Haxby, J.V. Distinct representations of eye gaze and identity in the distributed human neural system for face perception. *Nat. Neurosci.* **3**, 80–84 (2000).

## ONLINE METHODS

Participants in all experiments had normal or corrected-to-normal vision and received monetary compensation. The Vanderbilt University Institutional Review Board approved the experimental protocol and written informed consent was obtained from each participant.

**SiB experiment (Experiment 1).** Thirty-one right-handed individuals (12 females) participated. One individual's data were excluded owing to technical problems.

Participants searched for a target letter (X) in an RSVP stream of distractor letters (white Helvetica font,  $1.8^\circ \times 1.8^\circ$ , presented on a dark gray background). Each 8-s trial began with a 3.4-s RSVP of 31 letters randomly chosen from a set of 20 (vowels were excluded), with no letter presented twice in a row. Each stimulus was presented at fixation for 100 ms followed by a 10-ms inter-stimulus interval (ISI). Following the RSVP, a screen appeared for 2 s prompting the participants to respond with an appropriate key press (right index finger for 'target present' and right middle finger for 'target absent'). The response period was followed by a 2.6-s ITI consisting of a white fixation cross.

Each participant completed a single fMRI run of 40 trials. The target (present on 77.5% of trials) appeared between frames 25 and 29. In six of the trials, a surprise stimulus (grayscale face,  $1.8^\circ \times 1.8^\circ$ , distinct for each trial) appeared between frames 22 and 26 of the RSVP, 330 ms before the target (5 trials) or in a trial with no target (1 trial). Surprise trials occurred between trials 2 and 38 and were separated by a minimum of two search trials (trials with a target but no surprise stimulus). Participants practiced search trials exclusively before the fMRI session. Feedback was given only during practice, and participants were required to reach target accuracy above 80% before scanning. At no time were participants informed about the surprise stimuli.

To assess the effect of repeated surprise stimulus presentations, we used Cochran *Q* tests for categorical data of dependent samples<sup>47</sup>. We then applied sign tests to determine the significance of the relevant pair-wise comparisons. These and all subsequently described tests were two-tailed with  $\alpha$  at 0.05 unless otherwise noted.

Anatomical 3D high-resolution images were acquired using conventional parameters on a 3T GE MRI system. Nineteen 7-mm-thick axial slices (0 mm skip;  $3.75 \times 3.75$  mm in-plane) were taken parallel to the anterior commissure–posterior commissure (AC–PC) line. T2\*-weighted image parameters: 25 ms echo time, 70° flip angle, 240 mm FOV,  $64 \times 64$  matrix, 2,000 ms repetition time. The functional scan included 166 brain volumes, with the first 6 volumes discarded for signal stabilization. Trials were presented using Psychophysics Toolbox<sup>48,49</sup> for Matlab on an Apple G4 Macintosh. Stimuli were back-projected from an LCD projector onto a screen viewed through a prism mirror by the supine participant.

Data analysis was performed using BrainVoyager 4.9.1, BrainVoyager QX 1.7.9 (Brain Innovation), and custom Matlab software. Data preprocessing included image realignment, 3D motion correction, linear trend removal and correction for slice acquisition timing. Statistical parametric maps (SPMs) of BOLD activation were created using a multiple regression analysis, with regressors defined for the six surprise stimuli, search trials, and no-target trials; boxcar functions for each trial type were convolved with a canonical double- $\gamma$  hemodynamic function (SPM2, <http://www.fil.ion.ucl.ac.uk/spm>) to generate each regressor. The resulting maps from all participants were spatially smoothed with a 6-mm Gaussian kernel (full width at half maximum), standardized to Talairach space<sup>45</sup>, and superimposed to create composite maps. The model fit was assessed using *t* statistics, with significance determined by the false discovery rate (FDR) threshold at  $q < 0.05$  (random-effects analysis).

For the group region of interest (ROI) analysis, the center of mass and surrounding activated voxels for each activated focus were selected, up to  $1 \text{ cm}^3$ . The time-course for each surprise trial was extracted from each ROI for each participant and then converted to percent signal change (baseline from the time point of surprise stimulus (SS) onset and two preceding points). The average time courses for pairs of SS (SS1+SS2, SS3+SS4, SS5+SS6) were computed for each participant. For statistical tests of amplitude, we identified the time point with the largest percent signal change between 6 and 8 s after surprise stimulus presentation for each SS pair for each participant, and then used paired *t*-tests for the appropriate comparisons.

For the individually-defined ROI analyses, we identified ROIs whose activity correlated with the performance of the primary target-detection task (SPM of open contrast of the predictor for search trials). Positive  $\beta$ -weights for the predictor were associated with the FEF, IPS and IFJ, whereas negative ones were associated

with the TPJ. Each ROI in each participant was defined as the peak voxel and significantly activated surrounding area up to  $1 \text{ cm}^3$ . Anatomical landmarks (FEF at the junction of the superior frontal sulcus and precentral sulcus; IPS in the intraparietal sulcus between  $y = -50$  and  $y = -70$ ; IFJ at the junction of the inferior frontal sulcus and precentral sulcus; TPJ around the posterior Sylvian fissure) were used to identify each region, consistent with earlier work<sup>3,5,13,44</sup>. We next extracted time courses for the surprise and search trials, creating baselines and averages as above. For statistical tests of amplitude, we compared the corresponding time points across a given pair of time courses using paired *t*-tests.

For statistical tests of activity onset timing, we first subtracted each participant's search trial activity from their surprise stimulus trial activity for the first pair (SS1+SS2), leaving activation specific to deficit-causing surprise stimuli. To estimate the hemodynamic response's onset time for these subtracted time courses, we employed a bootstrap approach<sup>50</sup> owing to the difficulty of acquiring reliable onset measures from each participant's pairs of surprise stimulus trials. Using linear interpolation, each participant's time courses, for both search-related (search trials) and surprise-related (surprise trials – search trials) activity, from each ROI were upsampled to 1-ms resolution and then smoothed with a Gaussian kernel (FWHM = 2 s). Thirty samples for each ROI were selected with replacement and averaged, a process that was repeated 10,000 times. For each of the resulting averaged samples, we computed the onset as the time when the time course had achieved 20% of its peak amplitude (results were similar for 10%). Finally, these onset values (10,000 per ROI) were compared across ROIs. For example, right IFJ onsets occurred before right IPS onsets for 9,977 of the samples. From this count, we computed a *P*-value, which in the example would be 0.0066, two-tailed. Interactions were computed by first subtracting the onset values for surprise-related activity from those for search-related activity and then comparing these differences across regions.

As no hemispheric differences were found in any of the above analyses, and to increase statistical power, we collapsed the data across hemispheres for all subsequent analyses.

The correlation analyses were performed on the data derived from the GLM analyses after further processing steps had been applied. Global signal fluctuations in this dataset were removed by regressing out the time courses from a ventricular region of interest, a white matter region of interest, and the average signal across the entire brain. Second, the data were filtered using a zero-phase forward and reverse band-pass filter ( $0.01 < f < 0.2$  Hz). Next, we segmented the data from each individually defined ROI by trial, performing a percent signal change transform on each trial as described above. Trials were then concatenated by condition, yielding 28 points associated with surprise trials (SS1+2) and 28 points with search trials (two randomly selected trials from about 10 that were at least three trials away from any surprise trials). Time courses for each ROI (collapsed across hemispheres) pair of interest in each participant were then correlated by condition and the resulting values converted using Fisher's *z* transformation. The correlations between regions were then tested for significance across participants with one-sample *t*-tests, and the change in correlations between search and surprise trials compared across participants with paired *t*-tests.

**Spatial SiB experiment (Experiment 2).** Six right-handed individuals (three females) participated. The timing of each trial was as in Experiment 1 except that 29 stimuli were shown on each trial and the ISI was 17 ms. There were 40 trials during each of six fMRI runs. The target (present on 80% of trials) appeared between frames 23 and 27. In four of the trials per run (three target-present and one target-absent), a surprise stimulus appeared 350 ms before the target at one of four spatial locations centered  $4.2^\circ$  from fixation. The surprise stimuli consisted of distinct, large ( $6.5^\circ \times 6.5^\circ$ ), colorful items, each shown only once. Surprise trials occurred between trials 2 and 38, and were separated by a minimum of three search trials. Participants practiced the search task before the fMRI session. Participants were not informed about the surprise stimuli.

Anatomical 3D high-resolution images were acquired using conventional parameters on a 3T Philips MRI system. Thirty-three 3.5-mm thick axial slices (0.5 mm skip;  $1.875 \times 1.875$  mm in-plane) were taken parallel to the AC–PC line. T2\*-weighted image parameters: 35 ms echo time, 79° flip angle, 240 mm FOV,  $128 \times 128$  matrix, 2,000 ms repetition time. There were 161 brain volumes per functional scan. Trials were presented using Psychophysics Toolbox<sup>48,49</sup> for Matlab on an Apple MacBook Pro, and stimuli back-projected to the participant as in Experiment 1.

Data analysis was performed using BrainVoyager QX 1.11.4 (Brain Innovation) and custom Matlab software. Data preprocessing, SPM generation, ROI definition and event-related average construction were identical to the methods in Experiment 1.

We used a bootstrap analysis to test the hypothesis that the delay in dorsal network activity (relative to the ventral network) was significantly greater in Experiment 1 than in Experiment 2. After constructing bootstrap samples, we obtained the onset measures for the search-related and surprise-related activity for each ROI in each experiment. To increase power, we collapsed these measures across hemispheres and network nodes (dorsal or ventral). We then compared the onset measures for Experiment 1 ( $(\text{Search} - \text{Surprise})_{\text{Dorsal}} - (\text{Search} - \text{Surprise})_{\text{Ventral}}$ ) with those for Experiment 2 (same subtractions). As the 90% confidence intervals for the resulting metrics did not overlap, the comparison was significant one-tailed at  $P < 0.05$ .

**Endogenous cueing task experiment (Experiment 3).** After completing Experiment 2, the same six individuals participated in Experiment 3 during the same scan session.

Each trial began with a central dot ( $0.25^\circ$  in diameter) changing from white to either green or blue for 2,000 ms, which indicated in which of two squares ( $1.0^\circ$  across, located  $3.4^\circ$  right or left of fixation) an upcoming target was likely to appear (81% validity). The cue's color-location mapping was counterbalanced across participants. The target, a white dot ( $0.25^\circ$ ) that appeared inside one of the boxes for 100 ms, was presented 4, 6, 8 or 10 s after the cue onset. The frequency

of each delay period was exponentially distributed to maximize deconvolution efficiency. Participants responded to the target with a speeded button press. The next trial commenced after an ITI of 4–10 s (exponentially distributed). Participants completed 32 trials during each of 3 runs.

One participant's behavioral responses were not collected owing to a technical error, and another participant performed the task incorrectly by withholding responses to invalidly cued targets. Behavioral data for these two individuals were collected during a separate session outside the scanner.

The imaging procedure was identical to that used for Experiment 2.

After employing the same preprocessing steps used for Experiment 2, time courses from Experiment 2's search task ROIs were constructed using a deconvolution analysis.  $Z$ -transformed  $\beta$ -estimates, corrected for serial autocorrelations, were derived for the 10 volumes following the cue onset and for the 10 volumes following target onset, and individual time courses were averaged across participants and hemispheres (Fig. 5b). To test for significant activation in each region, one-sample  $t$ -tests were performed on the average of the third and fourth volumes after cue onset.

47. Sheskin, D.J. *Handbook of Parametric and Nonparametric Statistical Procedures* 2nd Ed. (CRC Press, Boca Raton, Florida, 2000).
48. Brainard, D.H. The psychophysics toolbox. *Spat. Vis.* **10**, 433–436 (1997).
49. Pelli, D.G. The VideoToolbox software for visual psychophysics: transforming numbers into movies. *Spat. Vis.* **10**, 437–442 (1997).
50. Davison, A.C. & Hinkley, D.V. *Bootstrap Methods and Their Application* (Cambridge University Press, Cambridge, 1998).